

Geohazards related to Karst and slope instability along, the Safaga-Gabal EL-Zeit area, Red Sea Coast, Egypt

Bosy A. El-Haddad^{1*}, Ahmed M. Youssef^{d,2}, Abdel-Hamid El-Shater¹ and Mohamed H. El-Khashab¹

1 Geology Department, Faculty of Science, Sohag University, Sohag, 82524, Egypt

2 Geological Hazards Department, Applied Geology Sector, Saudi Geological Survey, P.O. Box 54141, Jeddah 21514, Kingdom of Saudi Arabia,

Received: 23 Jan. 2022, Revised: 12 Apr. 2022, Accepted: 24 Apr. 2022.

Published online: 1 May 2022

Abstract: The Red Sea coast represents a vital sector of the Egyptian territory due to its economic and touristic activities. Different types of geohazard problems related to the karst features and slope instability were encountered in different areas along the Red Sea Coast. Karst features are very common in evaporite rocks due to their high susceptibility of dissolution as well as rock falls are distributed along the mountains and rock cuts that located in the vicinity of the roads and highways. The current study is aiming at identifying and mapping all the evaporite rock units and the slope instability sites along the Red Sea Coast stretch between Safaga and Gabal El Zeit, using medium and high resolution satellite images coupled with field investigations. Principal component analysis (PCA) and minimum noise fraction (MNF) were succeeded to map and isolate the evaporite units in the study area. 3D satellites images were used to investigate and extract the most hazardous slope instability sites. Our remote sensing findings were verified by field investigations.

Keywords: Geohazards – karst – landslides – evaporates – satellite images

1 Introduction

The Red Sea coast stretch considers being a vitally important in Egypt. This stretch is characterized by significant economic and touristic activities. Different types of geological hazards were encountered in Egypt such as landslides, karst, expansive soils, sand dunes, and flash floods [1]; [2],[3], and [4]. According to that the Red Sea stretch has attracted the interest of researchers over the past few decades due to the crucial importance of this area. These studies were covering a wide spectrum of research such as geological units, structural studies, and geological hazards (e.g: [5], [6], [7], [8], [9]; and [10].

Remote sensing instruments measure reflected or emitted radiation in the visible, near-infrared, thermal infrared, and microwave portion of the electromagnetic spectrum. These data could be used to obtain information about the earth's surface from a distance. Different types of satellite images have been used in variou aspects such as identifying hydrothermal minerals, mapping structural elements and discriminationg of lithological units [11] and [12]. The arid and semi-arid types of environment are paradies for the application of remote sensing techniques.

Recently, there are some researches that have been interested in studying and assessment the different

geological hazards along the Red Sea coast area. However, the majority of these studies were concentrated on the flash flood hazards (e.g., [13]; [14]; and [15]). The evaporite rock units represent very susceptible rocks for the karstification process due to its high susceptibility of dissolution. Generally, the evaporite rocks have much higher solubility and faster dissolution rate than carbonates rocks and they are also have lower mechanical strengths [16]. The solubility of gypsum (CaSO₄.2H₂O) ranges from 2200-2600ppm in the temperature range of 0-40°C [17] and [18].

The current study aimed to identify and map the different geological hazards (karst and slope instability prone areas). In the current study medium and high spatial resolution satellite images, 3D images, and detailed field investigations were carried out along the Red Sea coast stretch between Safaga and Gabal El Zeit.

2 Study area

The study area is located in the east portion of Egypt along the Red Sea coast, extending from Safaga City to Gabal EL-Zeit (Fig. 1). The area has an arid climate, a mountainous topography on the west and Red Sea on the east. Little works have been accried out using remote sensing application in mapping of the different types of geohazards (karst and slope instabilities) in the study area. The Sohag-

* Corresponding author E-mail: bosy_abdelaziz@science.sohag.edu.eg

Red Sea highway in the study area is vitally important which connected the Nile Valley with the Red Sea cities. It cuts through rugged mountains for ~95km long (Fig. 1). This highway is under the risk of falling rocks (slope instability problem).

According to geomorphological point of view, the study area is divided into two main zones; 1) the Red Sea rugged mountains and 2) the coastal plain. Geologically, the study area is characterized by the presence of various rock units. These can be summarized from older to younger as follow; metavolcanic rock units; Dokhan alkaline volcanics, the Hammamt group (molasses-type sediments), the granitic rocks (younger granite and older granite), basic dyke swarms (trending NW-SE, and NE-SW) and sedimentary rocks (The Upper Cretaceous-Lower Tertiary succession including Dawi, Dakhla, Esna and Thebes formations and the Miocene rock succession including Um Mahara Formation, Abu Dabbab Formation, and Um Gheig Formation, Samadai Formation and Quaternary evaporites.

Evaporites in the study area are represented by two rock units; Abu Dabbab Formation and quaternary evaporites. Abu Dabbab evaporites in the area under study are composed mainly of gypsum, halite and poly-halite and anhydrite (Figs.2.A and B) [7] and [5]. Quaternary evaporites can be described as yellowish white anhydrite and gypsum (Figs.3.C and D) these evaporites are considered to be very hazardous rock units due to its high susceptibility of dissolution. The study area is dissected by different kinds of discontinuities (joints, faults, and folds) with different trends (NW-SE and NE-SW)

3 Data used and Methodology

In the current research, the materials used in this analysis consisted of Landsat 7 ETM+ imagery, acquired on 2016. Landsat7 ETM+ is multi-spectral remote sensing data which has 16 days temporal resolution. The image is cloud free and it is a geometrically corrected to a UTM Zone 36 north and WGS84 datum. The multi spectral image of the study area were prepared and enhanced its spatial resolution by the resolution merge technique; in order to produce 15m scene for the area under study. The ETM+ image with 15 m spatial resolution was subset to focus on the study area. The ETM+ was used to identify and map the karst prone areas (evaporite areas). The image processing has been done using the Environment for Visualizing Images (ENVI 5.0) software. To map the karst prone areas (evaporites rock units) in the study area, different image processing modules were implemented. Two areas were selected to apply these techniques including Gabel El-Zeit area (Site No. 1) and North of Safaga port at wadi Abu Nakhra (Site No. 2) (Fig. 1). These techniques include: (a) false color composite (bands 742 in RGB) and (b) advanced techniques including the principal component analysis (PCA) [19] and the minimum noise fraction (MNF) transformation [20]

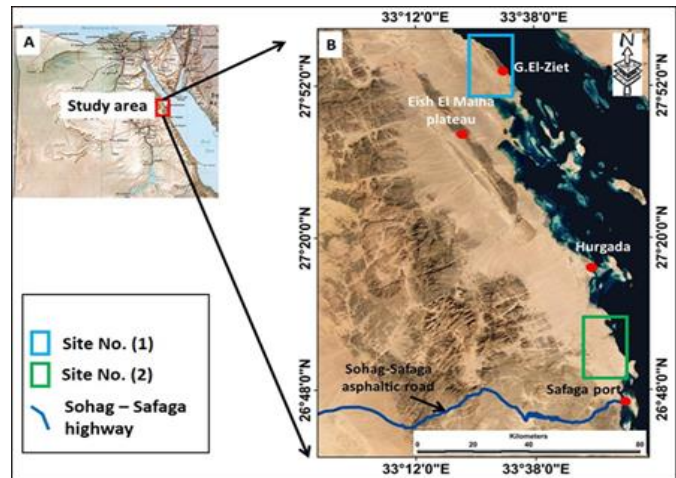


Fig.1: (A) Study area location in Egypt map; (B) Detailed characteristics of the study area

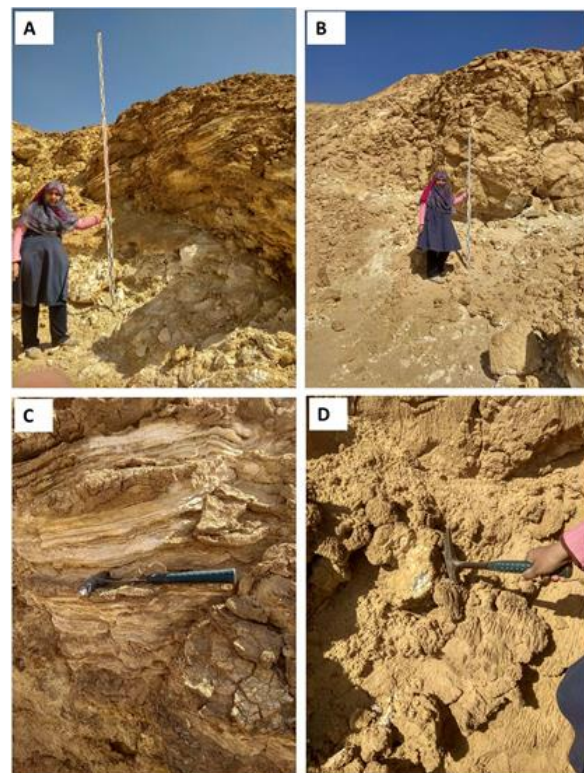


Fig.2: A) and B) show evaporites rock units in the stud area.: A) and B) show the evaporites of Abu dabbab Fm in Site (No1), and C) and D) Show the quaternary evaporites patches at site (No2).

Different types of remote sensing data are very helpful in detecting surface features related to slope instability phenomena such as using very high resolution satellite images using professional Google Earth images, Esri data, Digital Glope, GeoEye, Earthstar Geographics, and CNES/Airbus) with 1 meter resolution or less. In the current study, the Google Earth high resolution image was used to generate the 3D perspective view to map and identify the slope instability vulnerable areas. Lineaments in

the study area were extracted from digital elevation model DEM (30 m resolution) and other remote sensing filtering techniques. Also, the correlation between the dominate trends of lineaments and probability of rock falls in the study area was identified. ArcGIS 10.2 and Rock Work 14 programs were used to indicate the main trends of lineaments in the study area.

The results have been verified with the field investigations. Field investigations help in verifying the remote sensing results) and the 3D model results.

4 Results and Discussions

4.1. Mapping the evaporite rocks (Karst susceptible areas)

Due to the high susceptibility of dissolution of evaporites, mapping of all exposed evaporites deposits in the study area became necessary to complete the karst hazards assessment. From the detailed study of different geologic maps and previous literatures of the study area, we conclude that the evaporites deposits in the study area are restricted to the coastal area

A false color composite image (bands 742 in RGB) has been prepared for the study area (Fig. 3). The result of this data shows a little distinction between evaporate rock units and the surrounding rock units. In the image, the evaporite unit could be distinguished easily which appears in Cyan color. False color composite (742) in RGB to discriminate the evaporites sediments from the surrounding rocks[2].

Advanced enhanced techniques were applied principle component analysis (PCA) and minimum noise fraction (MNF). The purpose of using these advanced techniques in the present study is to identify the suitable composite band combinations that can enhance the identification of the karst prone rocks from the surrounding materials. Our results indicated that in minimum noise fraction (MNF) bands 243 in RGB discriminate the evaporite sediments from its surroundings (Fig.4). The evaporite rocks appeared with dark violet color. In PCA image with combination bans 432 in RGB the evaporite rocks appeared with bright cyan color (Fig. 5).

A detailed field investigation was conducted to verify and examine the different karst features in the evaporite rock units in the two selected sites (Gabel El-Zeit area (Site No. (1)) and North of Safaga port at wadi Abu Nakhra (Site No. (2))

Fig.2: A) and B) show evaporites rock units in the study area.: A) and B)show the evaporites of Abu dabbab Fm in Site(No1), and C) and D)Show the quaternary evaporites patches at site (No2).

Site (No. 1) evaporites: it represents Gabal El-zeit area, which is characterized by the presence of Abu Dabbab Formation. It is mainly composed of gypsum, halite, poly-

halite and anhydrite. It extends along the western edge of Gabal El-Zeit for about 27 km as several low lying hills (7 to 15m high). Abu Dabbab Formation (Middle - Late Miocene Evaporites) were classified into several facies, includes the thinely bedded calcium sulphate facies, laminated evaporites, nodular evaporites sulfatized carbonate facies and selentic gypsum facies [23]. These different types of facies were identified in the field where stromatolite –evaporite facies, thinly bedded facies, laminated facies and massive facies are appeared in (Fig. 5A to E). In addition to that different karst features were observed in Gabal El-zeit area such as, sagging features, open cavities, and detached blocks due to the dissolution processes (Fig. 5F to H).

Site (No. 2) evaporites: it includes Wadi Abu Nakhra area, it is characterized by circular and oval patches of evaporites, and name as quaternary evaporites were recorded in the study area north the Safage cite at Wadi abu Naukhra. Theses evaporites filled of different depressions near the Red Sea coast. Field investigation showed that these patches are massive evaporites, which exposed at the surface (Fig. 6). These patches are subjected to dissolution and collapsing susceptibility at high rates. Some of these areas are located in and close to new tourist resorts which may cause some geological hazards due to the presence of karst features.

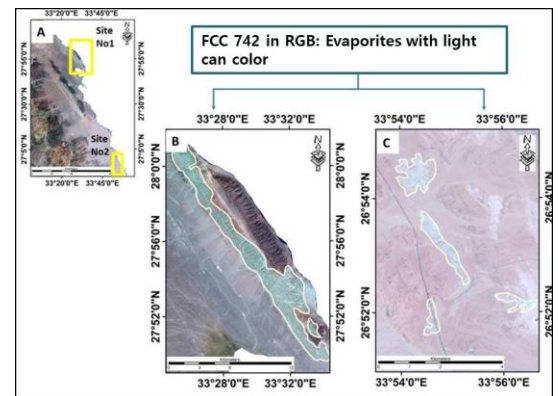


Fig.3: A) Shows a false color composite (bands 742 in RGB) for the coastal part of the study area where the evaporites appear in light cyan color, (B and C) are close up view for sites (1, 2) respectively.

4.2. Mapping of slope instapilty sites in the Red Sea rugged mountaounous basement along Sohag- Safaga asphaltic road:

In this part of the study we used the modern techniques and the high resolution satellite images to indicate with a great accuracy the potential slope instability sites. We generate 3D images from the Googel Earth Professional data to extract the different features of the slope instability in this part of the study area such as hanging blocks and unstable dangerous vertical cliffs. We also found that the different high resolution satellite images are very helpful in extracting the different direction of lineaments in the rock units in the hazardous sites.

lineaments is the main source of generating the different hanging blocks and rock fall.

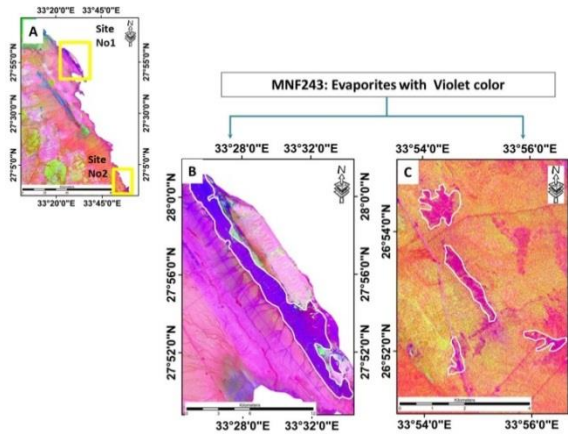


Fig.4: A, B, C) Shows MNF (243 in RGB) for the coastal part of the study area where the evaporites appear in violet color. B and C) Show close shots for site No. (1) and No. (2).

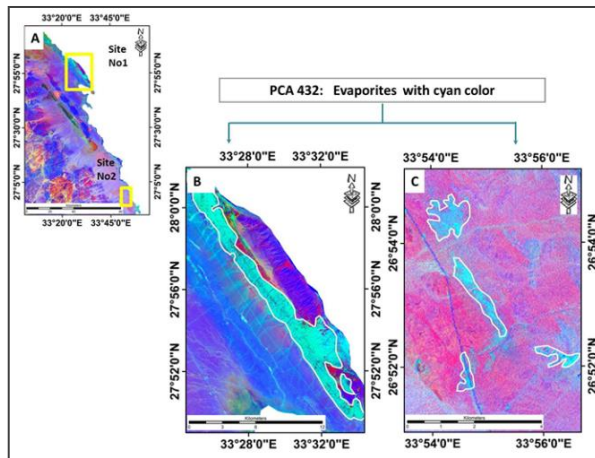


Fig.5: A, B, C) Shows PCA (432) in RGB for the coastal part of the study area where the evaporites appear in cyan color, B and C) Show close up views for site No. (1) and site No. (2).

The 3D satellite images enable us from covering a very wide area and extracting all dangerous slope instability sites along the Sohag-Safaga road and also from understanding the most important factors which control and trigger the slope instability problems generating along the asphaltic road.

The current study succeeded to extract 63 sites along Sohag-Safaga asphaltic road (Fig.3.A). Several slope instability features are indicated using the 3D images, such as hanging blocks and dangerous unstable cliffs (Figs.6,B,C,D), (Fig.7.A and B) and (Figs.8. A and B). From the detailed visual interpretations of the 3D satellite images, we noticed that the different hanging blocks and unstable cliffs are controlled directly with the trends of the different lineaments (Figs.6.B,C,D and E), so it was a priority in this section of our study to extract the different trends of lineaments in this part of the study area. The main directions of lineaments in this part of the study area are NE and NW. The intersection of the different directions of

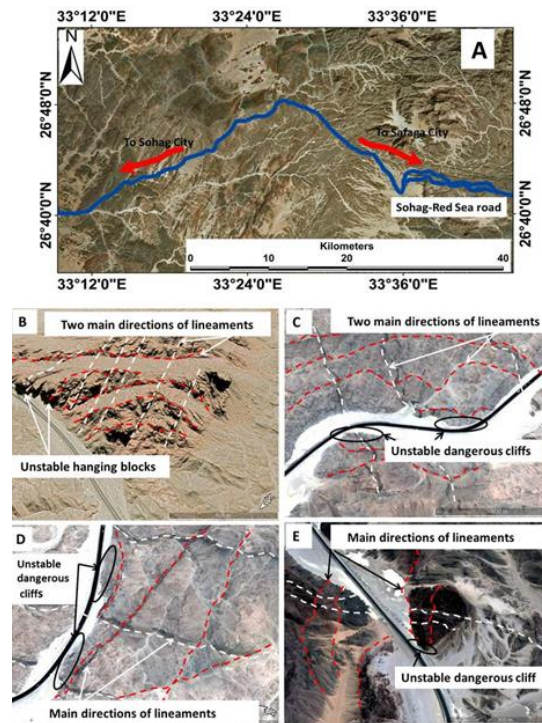


Fig.6: (A) a location map for the Red Sea rugged mountainous basement along Sohag-Safaga asphaltic road. (B),(C),(D) and (E) show different slope instability sites such as unstable hanging blocks and unstable cliffs and the main directions of lineaments along the asphaltic road.

The next step after mapping the most hazardous slope instability sites in this part of the study area, is to examine the accuracy of the remote sensing results by several field trips. All the 63 sites were visited and we compared the 3D images results with the field investigations data and identifying the different factors which trigger the slope instability in this part of the study area. The results proved that all the mapped sites are represent very hazard slope instability sites. Also, we measure the different directions of joints and fractures in these sites to confirm the results of remote sensing data. In (Figs. 7and 8) we compare between the results of remote sensing and field investigations results.

From the detailed field investigation for the entire slope instability sites that we extracted from the high resolution satellite images, we found out that the frequency and the directions of lineaments are essential factors in triggering the slope instability sites along the study area. The intersections of two or more directions of lineaments work on detaching the fallen rocks along the unstable cliffs in this part of the study area (Fig.6) and (Fig9). From the results of the field measurement we confirmed our remote sensing results of the lineaments directions.

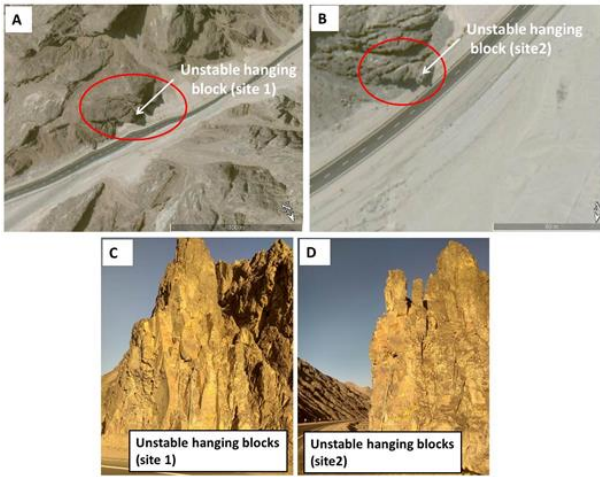


Fig.7: (A)and (B) show hanging blocks in site number 1 and 2 respectively along the asphaltic road in the 3D satellite images.(C)and(D) show how the hanging blocks in these sites appear in the field

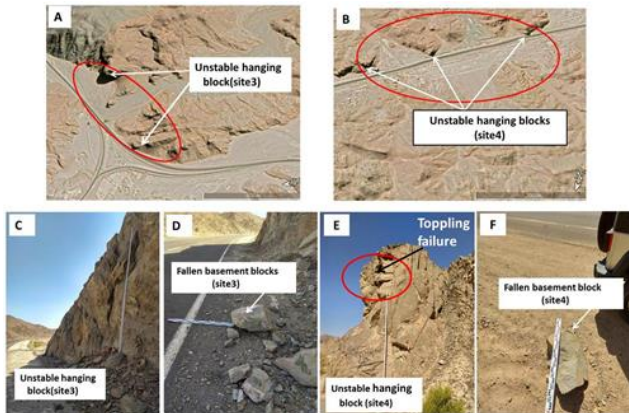


Fig.8: (A)and (B) show hanging blocks in site number 3 and 4 respectively along the asphaltic road in the 3D satellite images.(C)and (E) show how the hanging blocks in appear in the field. (D) and (F) the fallen basement blocks in sites number 3 and 4)

The main directions of fractures and joints are NE,NW and EW and we will discuss the lineaments and their trends in part of the study area in details in the next part. Another factor which controls of the degree of risk of the unstable cliffs and hanging blocks in this sector of the road is the width of the ditch of the asphaltic road. We could classify the slope instability sites according the width of the ditch into, moderate risk sites with ditch width ranges from 1-3 meters and high risk sites with ditch width less than 1 meter (Fig. 12) and from our results we found that the slope instability sites are restricted in three sectors (S1, S2 and S3) (Fig.10).Along this part of the part of the study area during the field investigations we recorded different slope failure types such as toppling, wedge and planner slope failure (Fig8.E), (Fig9.D and E)

Unfortunately, in most cases the ditch of the road is flat type, which increases the bouncing back of the fallen blocks on the road and destroying it in several cases and causing traffic accidents. The mapped slope instability sites were classified into 45 high risk sites with 71.4% from the total slope instability mapped sites and 18 moderate risk sites with 28.5% from the total mapped sites in this sector of the study area (Fig.16)

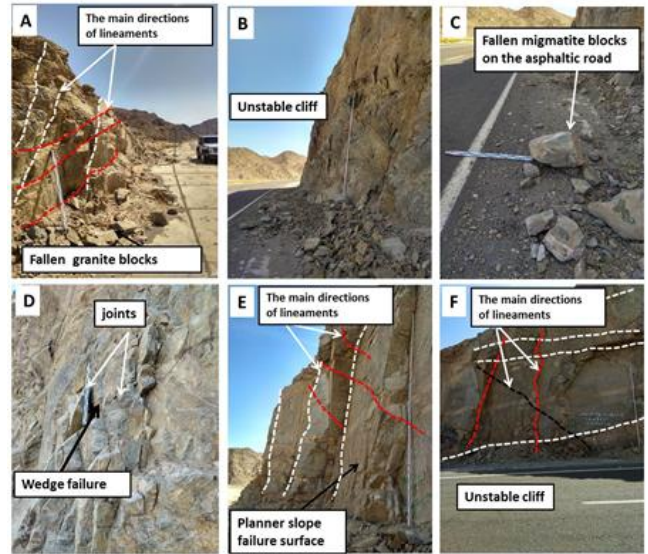


Fig.9: Different slope instability site.(A),(E) and (F) show the main directions of joints and fracture in different sites along the asphaltic road.(B) and (C) show unstable cliff, and fallen migmatite blocks on the asphaltic road. (D) and (E) show wedge and planner slope failure respectively

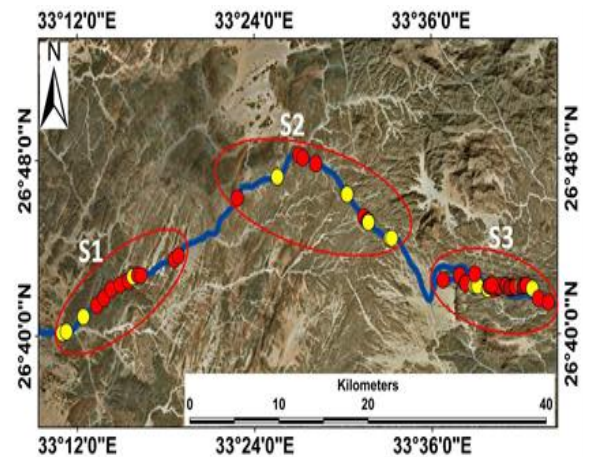


Fig.10: Shows the distribution of the slope instability sites. The high risk sites with red points and the moderate risk sites with yellow points. The slope instability sites are accumulate in three sectors, S1,S2 and S3

4.3.2. Application of remote sensing data for lineament extraction:

From the previous results we understand that the different linear features are the essential factor which control the development of the different slope instability features. We used three different sources of remote sensing data which are; (1) very high resolution images prepared by Esri from Digital Globe, GeoEye, Earthstar Geographics, CNES/Airbus combinations with spatial resolution less than 1 meter, (2) digital elevation model DEM generated from SRTM data 90 m spatial resolution and (3) Landsat7 ETM+. In order to enhance our opportunity in lineaments extraction from Landsat images, Landsat7 ETM+ data has been used with the help of some spectral enhancement techniques (Filtering techniques) (Figure.14) to improve the ability of detecting lineaments features we used the directional filter with an angle of (315°) which found very helpful in lineaments extractions by [22].

To analyze these lineaments, Arc GIS 10.2 and Rock Work 14 have been used. Arc GIS used to create the attributed table for all these lineaments and extract start, mid, and end points coordinates for each line. Rockworks 14 have been used to analyze this attribute table and prepare the bearing values for each lineament line then draw a rose diagram for all this part of the study area and for each sector from the three sectors which were indicated previously.

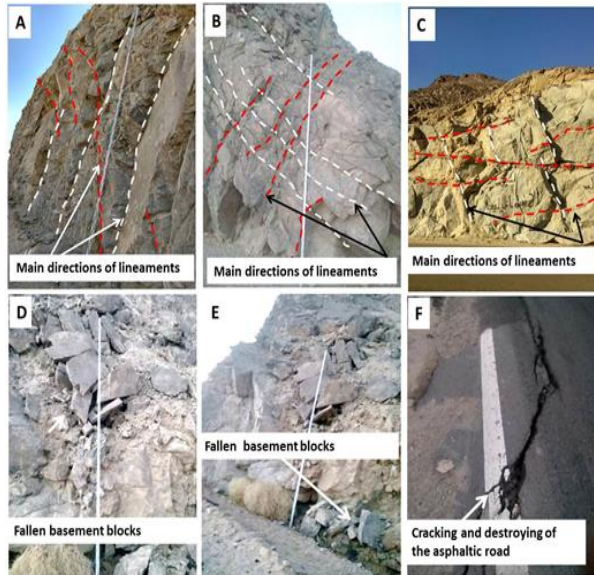


Fig.11: Different sites of slope instability hazards along Sohag-Red Sea asphaltic roads. (A),(B) and (C) show the main directions of joints and fractures. (D) and (E) the deformation and fragmentation of the host rocks and fallen blocks due to this deformation. (F) shows the destroying of the asphaltic road due to the repeated rock fall in site.

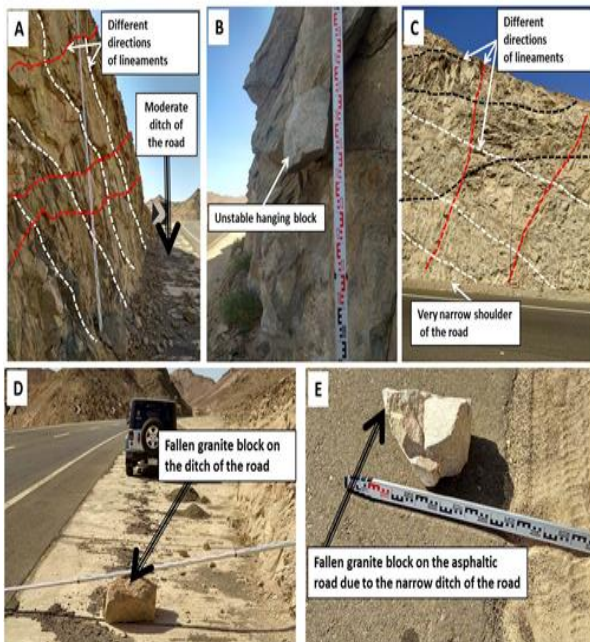


Fig.12: different sites of slope instability hazards along Sohag-Red Sea asphaltic roads. (A)and(C) show the different direction of lineaments in unstable cliffs. (B) shows an unstable hanging block as a result of the intersection of the different trends of lineaments. (D) shows a fallen granitic block on the wide ditch of the road and (F) shows a fallen granite block directly on the asphaltic road due to the very narrow ditch of the road (less than 1 meter)



Fig.13: Different sites of slope instability hazards along Sohag-Red Sea asphaltic roads. (A) a very narrow and flat ditch of the road(B) and (F) show planner and wedge slope failure. (C) a very large unstable hanging granite blocks.(D) and (E) show different sizes of fallen basement blocks on the asphaltic road.

Our results proved that the main trends for the whole area is NE and NW (Fig15). In sector (1) which contains 14 sites of slope instability sites (22%) the main directions of lineaments are NE and NW (Fig.16.A). Sector (2) have the same number of slope instability sites and the main trends of lineaments are NE and ENE (Fig.16. B). Sector (3) which has 35 of slope instability sites with a percentage reach 55% from the total number of the dangerous slope instability sites. The analysis of the lineaments trends in sector(3) explains the cause of this high percentage. The results show that in sector (3) there are several common trends such as NE,EW,NNW and NW (Figure16.C). The excess in the main trends in this sector increases the number of the intersections of the linear features. These intersections play an essential role in development the different slope instability sites.

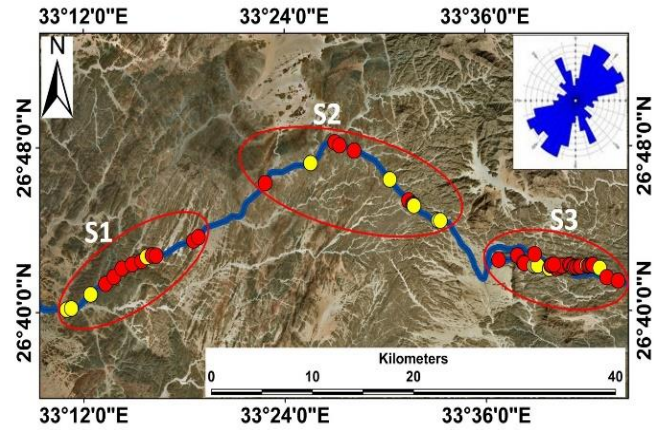


Fig.15 shows the extracted linear features of the area around the Red Sea rugged mountainous basement along Sohag- Red Sea asphaltic road. (B)The rose diagram shows the main trends of linear features in this part of the study area. The slope instability sites are accumulate in three sectors, S1,S2 and S3 with red shapes.

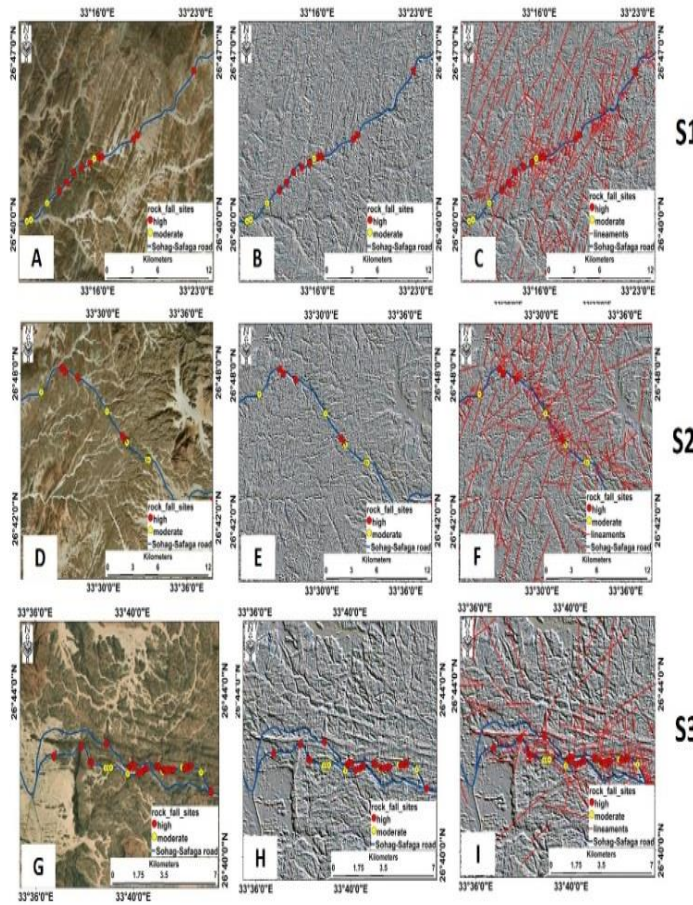


Fig.14: The sequential steps to extract linear structures in this part of the study area. (A),(B) and (C) high resolution satellite image, directional filter with (315°) and the extracted lineaments in sector 1. (D), (E) and (F) high resolution satellite image, directional filter and the extracted lineaments in sector 2.(G), (H) and (I) high resolution satellite image, directional filter and the extracted lineaments in sector 3.

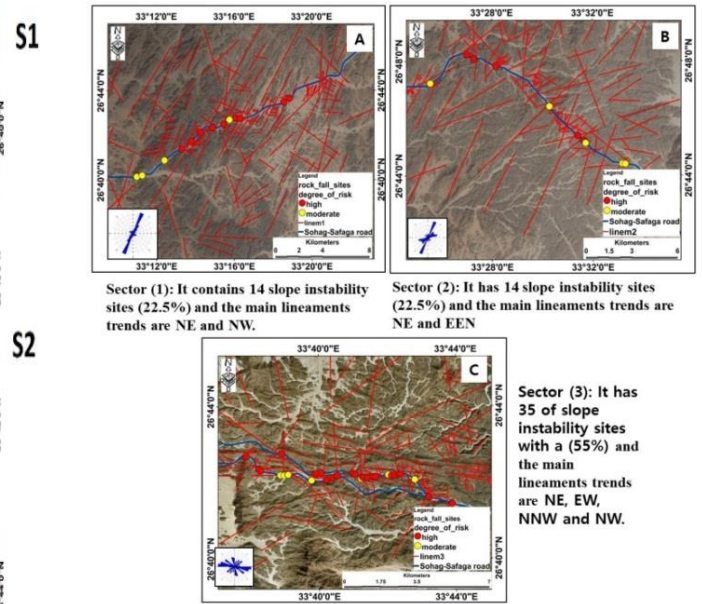


Fig.16: Shows the extracted linear features and the rose diagram for each segment

Conclusion

The different remote sensing techniques coupled with detailed field investigations were found as very effective, low cost modern strategy to detect all site of the geological hazards which are related to the different slope instability and the different karst and slope instability features. Also we indicate the different factors which control the different geo- hazards in the study area to conduct several percations must have been considered during the planning of any

development projects or transportation lines in the study area.

Recommendations

Mapping the potential sources slope instability sites is very important procedure in order to protect the highways and/or infrastructures from rock fall problems. Generation of a potential slope stability hazard map could be easily developed from the 3-D-high resolution satellite image and field investigations.

There are different methods of remediation/mitigation strategies could be suitable for the study area including: rock removal methods, using restraining, rock bolting and wire mesh and shotcrete, increasing ditch capacity, Jersey barriers, and draped mesh.

References

- [1] B.A.El-Haddad,, A.M. Youssef, A. El-Shater, and M. H. El-Khashab (2017)."Slope Stability Hazard Assessment Using 3D Remote Sensing and Field Sketching Techniques Along Sohag-Red Sea-Cairo Highway, Egypt." *Advancing Culture of Living with Landslides: Volume 2 Advances in Landslide Science* 407.
- [2] A. M. Youssef, B. A. F. Pradhan, D. Gaber, and M. F. Buchroithner. (2009)"Geomorphological hazard analysis along the Egyptian Red Sea coast between Safaga and Quseir." *Natural Hazards and Earth System Sciences* 9, no. 3 751-766.
- [3] A. M. Youssef, B.A.F. Pradhan, A. A. Sabtan, and H. M. El-Harbi. (2012) "Coupling of remote sensing data aided with field investigations for geological hazards assessment in Jazan area, Kingdom of Saudi Arabia." *Environmental Earth Sciences* 65, no. 1: 119-130.
- [4], A. M. Youssef, A. El-Shater, M. H. El-Khashab, and B. A. El-Haddad.(2017) "Coupling of field investigations and remote sensing data for karst hazards in Egypt: case study around the Sohag City." *Arabian Journal of Geosciences* 10, no. 11 : 1-13.
- [5] R. Said,, (1962) "The geology of Egypt": Elsevier Pub. Co., Amsterdam, New York .
- [6] L.Dubertret, J.V.Hepworth, and F.M.Delany, (1970) Review of structural geology of the Red Sea and surrounding areas. *Philosophical Transactions for the Royal Society of London. Series A, Mathematical and Physical Sciences*: 9-20.
- [7] M.D. Samuel, and G.S. Saleeb-Roufaiel (1977) "Lithostratigraphy and petrographical analysis of the Neogene sediments at Abu Ghusun-Um Mahara area, Red Sea coast, Egypt". VEB Deutscher Verlag fur Grundstoffindustrie, Leipzig, p. 47-36.
- [8]M.F. ElRamly, and M.Hermira (1978) Geological map of the Aswan Quadrangle. Egypt.
- [9] S. M. Khalil and K. R. McClay, (2002) Extensional fault-related folding, northwestern Red Sea, Egypt. *Journal of Structural Geology*, 24(4),743-762
- [10] A. M. Youssef, B.A.F.Biswajeet,and E.Tarabees (2011) "Integrated evaluation of urban development suitability based on remote sensing and GIS techniques: contribution from the analytic hierarchy process." *Arabian Journal of Geosciences* 4, no. 3-4 463473.<https://journals.aom.org/doi/abs/10.5465/annals.2018.0057>,
- [11] M.H.Tangestani, and F. Moore (2001)"Comparison of three principal component analysis techniques to porphyry copper alteration mapping: a case study, Meiduk area, Kerman, Iran." *Canadian journal of remote sensing* 27, no. 2, 176-182.
- [12] Gupta, Nikhil, and Eyassu Woldesenbet. "Hygrothermal studies on syntactic foams and compressive strength determination." *Composite Structures* 61, no. 4 (2003): 311-320.
- [13] E.M.Ghoneim, N.W. Arnell and G.M. Foody(2002) "Characterizing the flash flood hazards potential along the Red Sea coast of Egypt". IAHS PUBLICATION, 211-216.
- [14] I. A. .El-Magd, E. Hermas, and M. El Bastawesy (2010) GIS-modelling of the spatial variability of flash flood hazard in Abu Dabbab catchment, Red Sea Region, Egypt. *The Egyptian Journal of Remote Sensing and Space Science*, 13(1),(81-88).
- [15] A. A.. Elnazer, S. A. Salman and A. S. Asmoay(2017) Flash flood hazard affected Ras Gharib city, Red Sea, Egypt: a proposed flash flood channel. *Natural hazards*, 89(3), 1389-1400.
- [16] F.Gutiérrez,A .H Cooper, K..S. Johnson (2008) Identification, prediction and mitigation of sinkhole hazards in evaporite karst areas. *Environmental Geology* 53: 1007–1022
- [17] Hardie, L.A. :The Gypsum-Anhydrite Equilibrium at One Atmosphere Pressure. *The American Mineralogist* 52 (January-February): (1967):pp.171-200.
- [18] C. W. Blount and F. W. Dickson,(1973) Gypsum-anhydrite equilibria in systems CaSO4-H2O and CaCO4-NaCl-H2O. *American Mineralogist: Journal of Earth and Planetary Materials*, 58(3-4_Part_1), 323-331.
- [19] A. P.Crosta, and J. M Moore (1989) "Geological mapping using Landsat thematic mapper imagery in Almeria Province, South-east Spain." *International Journal of Remote Sensing* 10, no. 3 : 505-514.

-
- [20] J. W. Boardman, F. A. Kruse, and R. O. Green. (1995) Mapping target signatures via partial unmixing of AVIRIS data.
- [21] A.A.El Haddad (1984) Sedimentological and geological studies on the Neogene sediments of the Egyptian part of the Red Sea. Unpubl. Ph. D. thesis (Assiut University, Egypt)DOI: <https://doi.org/10.31410/tmt.2020.441>.
- [22] B.A.El Haddad, (2014) Evolution of the geological history of the Egyptian Nile at Sohag area using sedimentological studies and remote sensing techniques(M. Sc. thesis, Geology Department, Faculty of Science, Sohag University, Egypt. 215+ 7 pp).
-